Extractant Aggregation

DOI: 10.1002/ange.201402677

Elucidation of the Structure of Organic Solutions in Solvent Extraction by Combining Molecular Dynamics and X-ray Scattering**

*Geoffroy Ferru, Donatien Gomes Rodrigues, Laurence Berthon, Olivier Diat, Pierre Bauduin, and Philippe Guilbaud**

Abstract: *Knowledge of the supramolecular structure of the organic phase containing amphiphilic ligand molecules is mandatory for full comprehension of ionic separation during solvent extraction. Existing structural models are based on simple geometric aggregates, but no consensus exists on the interaction potentials. Herein, we show that molecular dynamics crossed with scattering techniques offers key insight into the complex fluid involving weak interactions without any long-range ordering. Two systems containing mono- or diamide extractants in heptane and contacted with an aqueous phase were selected as examples to demonstrate the advantages of coupling the two approaches for furthering fundamental studies on solvent extraction.*

Metal recycling is a subject that has become topical owing to economic interests. As resources in chemical elements become worrying, and demand is expected to explode, it becomes crucial to recycle waste from mines, energy companies, and processing industries. The key step in recycling is separation, and liquid–liquid (LL) or solvent extraction remains one of the most suitable partitioning methods.[1] This method was developed for the separation of compounds on the basis of their different solubilities in immiscible liquids, usually water and an organic solution. Metal recovery is quite challenging owing to the poor solubility of inorganic ions in oils. The use of lipophilic complexing ligands is thus required first to complex target solute ions and second to solubilize the complexes within the oil phase. Most lipophilic extractant molecules have amphiphilic properties due to their dual structure made of a polar (the complexing group) and an apolar part (alkyl chains or hydrocarbon rings necessary to increase their solubility within the organic solvent).[2] It is now well-established that the organic phases involved in such processes are not molecular solutions of extractants, but rather structured solutions.[3] We propose herein that small- and wide-angle X-ray scattering (SWAXS) techniques can be used in combination with molecular-dynamics simulation to analyze the molecular and supramolecular structure of two organic phases.

Micellization phenomena in solvent extraction systems were considered first in 1991 by Osseo-Asare,[4] who described similarities between the behavior of surfactants and of the extractant molecules used in the PUREX nuclear process. Since then, the formation of reverse aggregates in aliphatic solvents has been highlighted with other types of extractants used for metal recycling in nuclear processes.[5] Moreover, the interactions between extractant aggregates within the organic phase are responsible for phase splitting[6] (such as the so-called third-phase formation, which is a major drawback in industrial processes and has a non-negligible impact on the separation efficiency). Usually, compact structures are identified, and the core diameter of the aggregates, often compared to reverse micelles, is less than 1 nm. Therefore, extractant molecules are always considered in the first or second coordination sphere of the extracted solutes.[7] At high concentration, or depending on the solute valence, the aggregates can grow in one or two directions.[8] However, despite the investigation of many systems, and despite the crossing of various techniques, such as X-ray or neutron scattering to probe the nanoscopic structures, osmometry to determine the chemical potential of the various species, and spectroscopy to characterize the coordination sphere of the extracted solutes, there is still no consensus on the large-scale supramolecular architecture of the aggregates, and more especially on their interactions, which are at the origin of phase instabilities.[2]

There are indeed several reasons for the difficulties encountered. For a solvent-extraction separation process, the extractant concentration in the oil phase is far above a critical aggregation concentration, which is already rather high owing to the strong affinity of the ligand for the solvent (in the range of $0.1\,\mathrm{M}$, whereas for a classical surfactant, the critical micellar concentration is usually below $5.10^{-3}\,\mathrm{M}$). Therefore, monomers coexist at a high concentration with aggregates.[5b,9] Moreover, the aggregates are small and characterized by a very low aggregation number (<10). Finally, owing to high local curvature of the interface between the polar core and the organic shell of these aggregates, some of the solvent molecules are embedded within the shell and so belong to the supramolecular structure. As a result, the contribution of the various species (solvent molecules, monomers, and various aggregates) to the different measurements is not easily distinguishable. Moreover, the strong

---

[*] Dr. G. Ferru, D. Gomes Rodrigues, Dr. L. Berthon, Dr. P. Guilbaud
DRCP/SMCS/LILA CEA Marcoule
30207 Bagnols-sur-Cèze (France)
E-mail: philippe.guilbaud@cea.fr

Dr. O. Diat, Dr. P. Bauduin
ICSM UMR 5257 (CEA/CNRS/UM2/ENSCM)
30206 Bagnols sur Cèze (France)

[**] This research was supported by the CEA (DSOE/RBPCH) and the scientific committee of the University of Montpellier II, as well as through national funding (ANR 12-BS08-0021; ILLA). We thank Eric Pellegrini for fruitful discussions on the simulation of the structure factors from MD simulations, as well as Bruno Corso for technical support with the SWAXS apparatus.

Supporting information for this article is available on the WWW under http://dx.doi.org/10.1002/anie.201402677.

dependence of the shape and size of the solvated complex on the chemical nature of both the extractant and the solvent, and also on the activity of the adjacent aqueous phase, makes it even more difficult to predict the final structure. A lack of detailed understanding of the structure and dynamics of this liquid supramolecular organization (in the bulk organic phase and at the interface between the two liquids) hampers the resolution of many cation-separation issues. Since no ideal or model system really exists, it is necessary to probe the behavior of each system of extractant molecules as a function of the required separation property: a difficult task.

To tackle this highly challenging issue, we crossed the results of molecular-dynamics (MD) simulations with those from scattering experiments and showed the pertinence of this approach in such a case. This combination has already been successfully used for other structured solutions, such as solutions of proteins,[10] ionic liquids,[11] hydrotropes in aqueous phases,[12] inverted micelles,[13] and detergentless microemulsions.[14] Both tools provide insight into the mixing properties at the nanometer scale in complex fluids and were used in this study to investigate the structure of two specific organic phases containing extractants. Small- and wide-angle scattering data were compared with the Fourier transform of pair correlation functions obtained from MD simulations with the program nMoldyn.[15]

Simultaneous detection of small- and wide-angle X-ray scattering (SWAXS) is convenient for the determination of the spatial variation of electronic densities from a few angstroms up to a few tens of nanometers, especially when the characteristic lengths of these fluctuations are small. The measured scattering intensity is proportional to the structure factor $S(\mathbf{q})$ or the Fourier transform of the radial distribution function that quantifies the excess probability density of finding a molecule near another molecule. $S(\mathbf{q})$ is an appropriate feature for comparing experiments and modeling and can be described as:

$$S(\mathbf{q}) = \frac{1}{N}\left\langle \left| \sum_{i,j} \rho_i \rho_j e^{-i\mathbf{q}(\mathbf{r}_i - \mathbf{r}_j)} \right|^2 \right\rangle$$

with $\mathbf{q}$ as the wave vector, ρ_i the scattering-length density of atom i (electron density for X-ray scattering), $\mathbf{r}_i$ its position vector, and N the number of diffusing sites.

The extrapolation value of $S(\mathbf{q})$ at $\mathbf{q} \rightarrow 0$ for a pure solvent is directly proportional to the compressibility of the fluid and is used for the normalization of the scattering intensity in absolute units (see the Supporting Information). In the scattering range covered by the instrument (see Figure 1, top) only the first oscillation in the structure factor is observed at large q-vectors.

The first chosen example concerns the *N*,*N*′-dimethyl-*N*,*N*′-dioctylhexylethoxymalonamide ligand (DMDOHEMA; see Figure SI.1 in the Supporting Information), an extractant molecule used to extract actinide(III) and lanthanide(III) cations from aqueous solutions in nuclear-fuel reprocessing.[16] Detailed analysis of the structuring of this system in different alkanes has been carried out as a function of water activity. Above a critical concentration of about 0.1 mol L^{-1} in heptane,[9d] an increase in the small-angle X-ray scattering signal was observed. This excess of scattering at low q-vectors for an extractant concentration of 0.6 mol L^{-1} is shown in Figure 1 (top; green curve) and can be compared to the scattering of the heptane solvent (black curve). This scattering excess gives us information on electron-density heterogeneities at the nanometer scale for this system, whereas the peak around 14.2 nm^{-1} corresponds to the first shell of the aliphatic chains in the solution, as in the pure solvent.

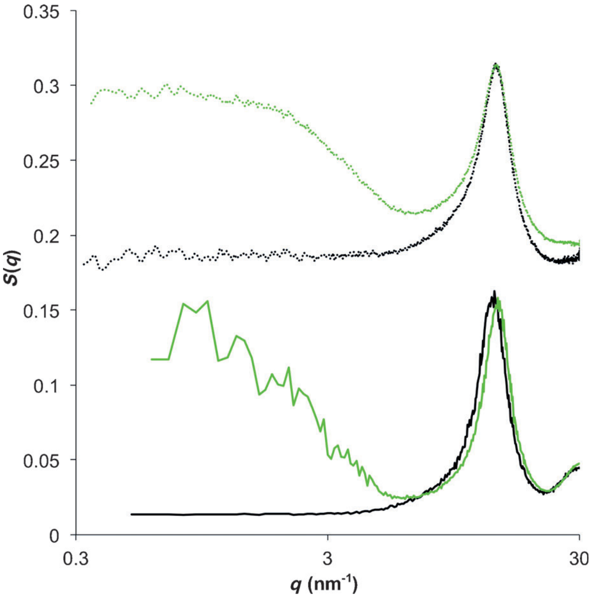

Figure 1. Comparison of the experimental (dotted lines) and theoretical (solid lines) SWAXS profiles obtained for pure *n*-heptane (black) and 0.6 M DMDOHEMA in *n*-heptane (green) after contact with pure water.

A classical analysis of the SAXS signal upturn (below 4 nm^{-1}), as developed in Ref. [17], can be applied to determine the size of these heterogeneities. The product of a form factor describing the shape of the malonamide aggregates and a structure factor that takes into account a sticky potential for characterizing the interactions of the aggregates enable us to simulate this intensity upturn. For malonamide in oil, spherical aggregates with a core size around 1 nm and aggregation numbers smaller than 10 have been determined as a function of the concentration.[18] However, this determination depends first on the geometrical hypothesis (spherical, ellipsoidal). It also depends strongly on the scattering contrast between the aggregate core, which is itself related to the number of trapped water molecules within the core and the salvation of the aggregate with heptane molecules within the shell. All these uncertainties are gathered in polydispersity parameters that are difficult to justify. Finally, the scattering simulation depends also on 1) the difference between the contributions of the spatial distribution of the monomer and the solvent, which remains difficult to quantify as a function of the extractant concentration, and 2) the crossed term taking into account the interferences between monomers and aggregates, which is not constant.

From molecular-dynamics simulations on the same system, as presented in Figure 1, there is clearly a dispersion

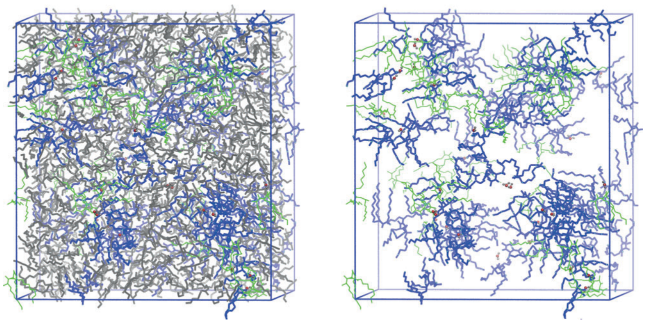

Figure 2. Molecular-dynamics simulation-box snapshot of the 0.6 M DMDOHEMA solutions, represented with (right) and without (left) the *n*-heptane solvent. Gray: *n*-heptane, green: DMDOHEMA monomers, blue: DMDOHEMA aggregates.

of the malonamide extractant molecules either in the form of monomers (Figure 2: green-colored malonamides) or within aggregates (Figure 2: blue-colored malonamides). These aggregates are not always formed around a cluster of water molecules (Figure 2: red and light-gray), but can be considered as rather compact and stable when they exist.[19] However, the ideal picture of a polar core surrounded by aliphatic chains and the solvent, as considered in classical SAXS analysis, does not appear in this simulation. The Fourier transform of the radial distribution functions presents a similar shape of the structure factor, characterized by an intense peak around 14.2 nm^{-1} and an upturn with a leveling off at lower q-vectors, as observed in the experimental data (Figure 1, bottom).

These simulations show that these aggregates are highly solvated by the heptane solvent and are in equilibrium with extractant monomers. At this concentration of 0.6 M, there is no signature of a long-range order nor of a network organization. Importantly, water molecules do not form a systematic anchorage point for micellization, as often mentioned when these aggregates are compared with reverse micelles.

From these MD simulations, it is possible to quantitatively partition the DMDOHEMA extractants into monomers (25 %), dimers (48 %), trimers (23 %), and tetramers (4 %). These data can be compared with those obtained from an analysis of vapor pressure osmometry (VPO) experiments under the same experimental conditions, that is, 0.6 M DMDOHEMA in *n*-heptane. The latter results suggested the presence of monomers (34 %) and tetramers (66 % of the extractants).[9d] The amount of extractant molecules in monomeric form is not too different (25 % as compared to 34 %); however, the distribution of aggregates with different aggregation numbers is more critical. These differences can be explained by the assumptions that are made to quantify the solvent-activity deviation and the much higher concentration range of the VPO measurements as compared to that used for calibration (see the Supporting Information). This comparison demonstrates the limits of the aggregation quantification deduced from VPO measurements. The above example shows the real contribution of the MD simulations to the supramolecular speciation of small polydisperse aggregates, which are difficult to quantify by a simple mathematical treatment of the VPO data.

A second example with another type of extractant molecule that is less amphiphilic was analyzed. Monoamides are a class of extractant with high affinity for uranyl molecules and whose interest was highlighted by Siddall in 1960.[20] By using the same approach as that for the malonamide, we performed MD simulations and SWAXS experiments for a monoamide (di(2-ethylhexyl)isobutyramide, DEHiBA) at two different concentrations (1 and 2 $\mathrm{mol\,L^{-1}}$) in heptane (Figure 3).

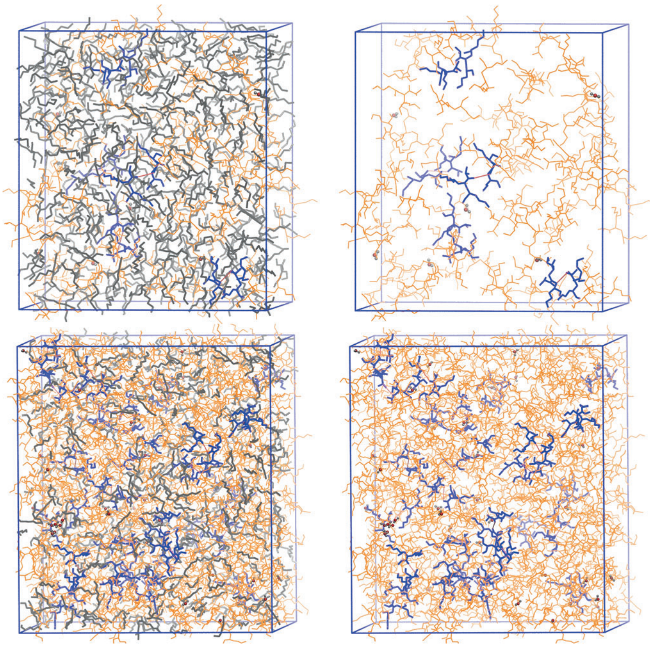

Figure 3. Molecular-dynamics simulation-box snapshots of the 1 (top) and 2 $\mathrm{mol\,L^{-1}}$ (bottom) DEHiBA solutions, represented with (right) and without (left) the *n*-heptane solvent. Gray: *n*-heptane, orange: DEHiBA monomers, blue: DEHiBA aggregates.

Contrary to the observations for the malonamide, the aggregation in this case seemed much less pronounced, whatever the extractant concentration. Mainly, monomers and dimers were found to be in equilibrium in heptane. Associated monoamides were in dimeric clusters, bonded either by dipole/dipole interactions or through water molecules. For the lowest extractant concentration (1 $\mathrm{mol\,L^{-1}}$), 82 % of the DEHiBA was in monomeric form, 17 % in dimeric form, and 1 % as trimers. At 2.0 $\mathrm{mol\,L^{-1}}$, the amount of extractant involved in aggregates increased (33 % in dimers and 4 % in trimers). In this highly concentrated system, the deviation between the VPO results and MD simulations was more significant: Although VPO analysis indicates that the amount of DEHiBA involved in dimers and trimers increases with the monoamide concentration, the amount of monomers was underestimated (59 and 30 % monomeric DEHiBA for 1 and 2 $\mathrm{mol\,L^{-1}}$ DEHiBA solutions, respectively).[21] Again, the VPO experiments were performed far from the ideal concentration range used for the osmometer calibration, which could explain these differences.

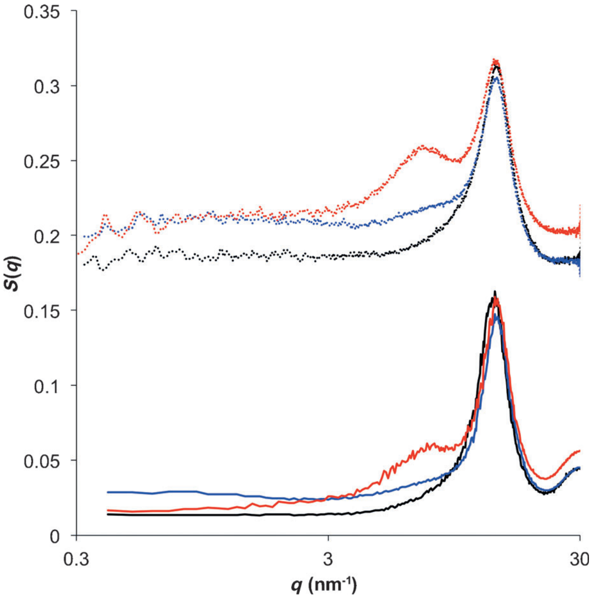

Figure 4. Comparison of the experimental (dotted lines) and theoretical (solid lines) SWAXS profiles obtained for pure *n*-heptane (black), 1 mol L^{-1} DEHiBA in *n*-heptane (blue), and 2 mol L^{-1} DEHiBA in *n*-heptane (red) after contact with pure water.

The simulated structure factors determined from these trajectories are presented in Figure 4 (bottom) and compared with experimental SWAXS data (top); in both cases, they are superimposed onto the structure factor of pure *n*-heptane (black curves). We can still recognize the peak at 14.2 nm^{-1} (first shell of the aliphatic chain). A second peak appears at 7.3 nm^{-1}. The intensity, but not the position, of this second peak depends on the monoamide concentration (see experimental SWAXS data with additional DEHiBA concentrations in Figure SI.2). This type of peak in the intermediate **q** regime was also observed in alcohol/water mixed solutions and was attributed to the correlation distance between alcohol OH groups. However, in that case, when alcohol molecules are diluted with water, the peak shifts towards lower q-vectors were analyzed in terms of swelling due to the hydration of the OH groups of alcohol molecules.[12,22] For the monoamide system, this peak is related to the correlation distance between the polar groups of the extractant molecules, a correlation which is quite strong and for which the distance does not change when the system is diluted with heptane. A logical explanation is that clusters formed by extractant molecules as dimers, trimers, or tetramers do not swell when heptane is added, but it is only the decrease in concentration that is related to the weakening of peak intensity, in agreement with MD simulations. For this second example, the contribution of the MD simulations is therefore also essential, since it allows speciation without the assumptions usually made for VPO or SWAXS data treatment, which depends on the experimental conditions.

In conclusion, we have shown that experimental SWAXS spectra of solutions containing extractant molecules in an apolar solvent can be accurately reproduced by MD simulation. This study specifically addressed for the first time the complex structure of the organic phase in solvent extraction with a quantitative description of the molecular and supramolecular organization of the extractant in oil at a wide range of concentrations. The classical fitting treatment applied to scattering spectra, for which the form and structure factors of dense aggregates dispersed in a homogeneous fluid are considered, has two major limitations that can be overcome by using MD simulation: 1) it cannot be applied at high extractant concentrations at which $P(\mathbf{q})$ and $S(\mathbf{q})$ cannot be decoupled, and 2) it is not valid in the high **q** range above 6 nm^{-1}, in which intermolecular distances become important. Therefore, the procedure proposed herein appears to be especially well-adapted for weakly aggregating amphiphiles,[23] such as hydrotropes[24] in water or lipotropes[25] in oils, which are typically characterized by high critical micellar concentration values and low aggregation numbers. Such systems are of high interest in various applied fields, and their aggregation process is still under debate.[26] We believe that these developments will have a significant impact on future investigations involving solvent extraction.

Received: February 21, 2014

Keywords: aggregation · amides · extractants · molecular dynamics · X-ray scattering

[1] C. Musikas, W. W. Schultz, J.-O. Liljenzin, *Solvent Extraction: Pinciples and Practice*, 2nd ed. (Eds.: J. Rydberg, M. Cox, C. Musikas, G. R. Choppin), Marcel Dekker, New York, **2004**, pp. 507–557.
[2] C. Bauer, P. Bauduin, J. F. Dufreche, T. Zemb, O. Diat, *Eur. Phys. J. Spec. Top.* **2012**, *213*, 225–241.
[3] a) M. P. Jensen, T. Yaita, R. Chiarizia, *Langmuir* **2007**, *23*, 4765–4774; b) F. Testard, L. Berthon, T. Zemb, *C. R. Chim.* **2007**, *10*, 1034–1041.
[4] K. Osseo-Asare, *Adv. Colloid Interface Sci.* **1991**, *37*, 123–173.
[5] a) S. A. Ansari, P. Pathak, P. K. Mohapatra, V. K. Manchanda, *Chem. Rev.* **2012**, *112*, 1751–1772; b) F. Q. Guo, H. F. Li, Z. F. Zhang, S. L. Meng, D. Q. Li, *J. Colloid Interface Sci.* **2008**, *322*, 605–610; c) M. Nilsson, K. L. Nash, *Solvent Extr. Ion Exch.* **2007**, *25*, 665–701; d) F. Testard, P. Bauduin, L. Martinet, B. Abecassis, L. Berthon, C. Madic, T. Zemb, *Radiochim. Acta* **2008**, *96*, 265–272.
[6] P. R. V. Rao, Z. Kolarik, *Solvent Extr. Ion Exch.* **1996**, *14*, 955–993.
[7] a) M. P. Jensen, A. H. Bond, *Radiochim. Acta* **2002**, *90*, 205–209; b) R. Chiarizia, K. L. Nash, M. P. Jensen, P. Thiyagarajan, K. C. Littrell, *Langmuir* **2003**, *19*, 9592–9599; c) M. P. Jensen, A. H. Bond, *J. Am. Chem. Soc.* **2002**, *124*, 9870–9877.
[8] P. Bauduin, F. Testard, L. Berthon, T. Zemb, *Phys. Chem. Chem. Phys.* **2007**, *9*, 3776–3785.
[9] a) L. Berthon, L. Martinet, F. Testard, C. Madic, T. Zemb, *Solvent Extr. Ion Exch.* **2007**, *25*, 545–576; b) H. Dozol, C. Berthon, *Phys. Chem. Chem. Phys.* **2007**, *9*, 5162–5170; c) R. J. Ellis, T. L. Anderson, M. R. Antonio, A. Braatz, M. Nilsson, *J. Phys. Chem. B* **2013**, *117*, 5916–5924; d) Y. Meridiano, L. Berthon, X. Crozes, C. Sorel, P. Dannus, M. R. Antonio, R. Chiarizia, T. Zemb, *Solvent Extr. Ion Exch.* **2009**, *27*, 607–637; e) S. Nave, G. Modolo, C. Madic, F. Testard, *Solvent Extr. Ion Exch.* **2004**, *22*, 527–551; f) R. J. Ellis, Y. Meridiano, R. Chiarizia, L. Berthon, J. Muller, L. Couston, M. R. Antonio, *Chem. Eur. J.* **2013**, *19*, 2663–2675.

[10] M. A. Jamros, L. C. Oliveira, P. C. Whitford, J. N. Onuchic, J. A. Adams, D. K. Blumenthal, P. A. Jennings, *J. Biol. Chem.* **2010**, *285*, 36121 – 36128.

[11] R. Hayes, S. Imberti, G. G. Warr, R. Atkin, *Phys. Chem. Chem. Phys.* **2011**, *13*, 3237 – 3247.

[12] M. Tomšič, A. Jamnik, G. Fritz-Popovski, O. Glatter, L. Vlček, *J. Phys. Chem. B* **2007**, *111*, 1738 – 1751.

[13] S. Abel, F. Sterpone, S. Bandyopadhyay, M. Marchi, *J. Phys. Chem. B* **2004**, *108*, 19458 – 19466.

[14] S. Schöttl, J. Marcus, O. Diat, D. Touraud, W. Kunz, T. Zemb, D. Horinek, unpublished results.

[15] K. Hinsen, E. Pellegrini, S. Stachura, G. R. Kneller, *J. Comput. Chem.* **2012**, *33*, 2043 – 2048.

[16] G. Modolo, H. Vijgen, D. Serrano-Purroy, B. Christiansen, R. Malmbeck, C. Sorel, P. Baron, *Sep. Sci. Technol.* **2007**, *42*, 439 – 452.

[17] C. Erlinger, L. Belloni, T. Zemb, C. Madic, *Langmuir* **1999**, *15*, 2290 – 2300.

[18] R. Chiarizia, M. R. Antonio, B. Gannaz, L. Berthon, N. Zorz, C. Hill, G. Cote, *Sep. Sci. Technol.* **2008**, *43*, 2572 – 2605.

[19] P. Guilbaud, T. Zemb, *ChemPhysChem* **2012**, *13*, 687 – 691.

[20] T. H. Siddall, *J. Phys. Chem.* **1960**, *64*, 1863 – 1866.

[21] G. Ferru, PhD Thesis, Université Pierre et Marie Curie (Paris 6), **2012**.

[22] a) P. A. Artola, A. Raihane, C. Crauste-Thibierge, D. Merlet, M. Emo, C. Alba-Simionesco, B. Rousseau, *J. Phys. Chem. B* **2013**, *117*, 9718 – 9727; b) F. Testard, P. Bauduin, T. Zemb, *J. Phys. Chem. B* **2008**, *112*, 12354 – 12360.

[23] T. Zemb, M. Duvail, J. F. Dufreche, *Isr. J. Chem.* **2013**, *53*, 108 – 112.

[24] P. Bauduin, A. Renoncourt, A. Kopf, D. Touraud, W. Kunz, *Langmuir* **2005**, *21*, 6769 – 6775.

[25] P. Bauduin, F. Testard, T. Zemb, *J. Phys. Chem. B* **2008**, *112*, 12354 – 12360.

[26] J. J. Booth, S. Abbott, S. Shimizu, *J. Phys. Chem. B* **2012**, *116*, 14915 – 14921.